

## ***Ab initio* Study on the Field Emission from Linear Carbon Chains and Carbon Nanotubes**

Seungwu HAN

*School of Physics and Center for Strongly Correlated Materials Research, Seoul National University, Seoul 151-742*

M. H. LEE and Jisoon IHM\*

*School of Physics, Seoul National University, Seoul 151-742*

(Received 9 November 2000)

We have performed first-principles calculations on the field emission of linear carbon chains and carbon nanotubes. The three-dimensional character of the current source, as well as the effect of the external electric field, are explicitly considered. The calculated electron-leakage graph is quite linear in short times, giving the tunneling rate from the emitter to the vacuum. The total current from the carbon chain fits the Fowler-Nordheim formula well. The magnitude of the current associated with each electronic state is found to exponentially depend on the energy level. In case of the unpassivated carbon chains, the dangling bond states pointing to the vacuum dominate the total current. We also study the emission currents from curved and tilted carbon nanotubes and find that a significant reduction in the emission current occurs compared with the case of the straight and vertical tubes.

Due to its high aspect ratio and the mechanical strength, the carbon nanotube [1] is regarded as a new material for the electron emitters to be used in the field emission display [2] as well as in the coherent electron source [3]. However, the emission mechanism of the nanotube is still not well understood and many unusual observations in the emission currents of carbon nanotubes remain to be explained [4,5]. In the early study on the field emission from open carbon nanotubes [6], it was suggested that the carbon chains ravelling from the nanotube edge induce remarkable changes in the emission current. In that experiment, the current was greatly quenched when the laser was illuminated on the nanotube and it was suggested that the elimination of the carbon chains at the end of the tube was the main reason for the significant current reduction. Theoretical studies on the electronic structure [7] and the emission current based on the WKB approximation [8] followed, and large sensitivities were found depending on the even-odd change of the number of constituent C atoms. Even though such carbon chains were not observed in the absence of the electric field [9], the understanding of the field emission mechanism from the carbon chain would provide a way to increase the performance of the nanotube as the electron emitter. Another interesting issue is that carbon nanotubes are usually curved or tilted

(with respect to the anode direction) in practical situations but the effects of these variations on the emission current are not precisely known.

Theoretical estimates of the emission current are usually done in a semi-classical fashion based on the Fowler-Nordheim (F-N) theory. The potential around the tip region is obtained by solving the classical electrostatics with the Laplace equation [10] or from the quantum mechanical calculations [8]. The transmission functions are then evaluated by using the one-dimensional semi-classical approach (*e.g.*, WKB approximation) along a specific line in the emission direction [11]. The electronic structure of the emitter is reflected in the supply function, as a form of the density of state. Such a simplified model, however, is not appropriate for the nanostructures. For instance, the boundary of the tip is not a well-defined physical quantity at the atomic scale and the potential obtained by solving the Laplace equation would not be valid for nanosize systems. In addition, the one-dimensional WKB calculation neglects any spatial variations of the wave function on the  $xy$ -plane (the emission is in the  $z$ -direction). Even for a flat metal plane, the suppression of the current from the  $d$  band compared to the  $s$  band has been well addressed in many works. [See Ref. 12 and references therein.] The situation becomes more complicated in the nanostructures where the  $xy$ -dimension of the tip is on the nanometer scale. It is also well-known that the total current changes significantly in the presence of the localized states induced by the

---

\*E-mail: jihm@snu.ac.kr

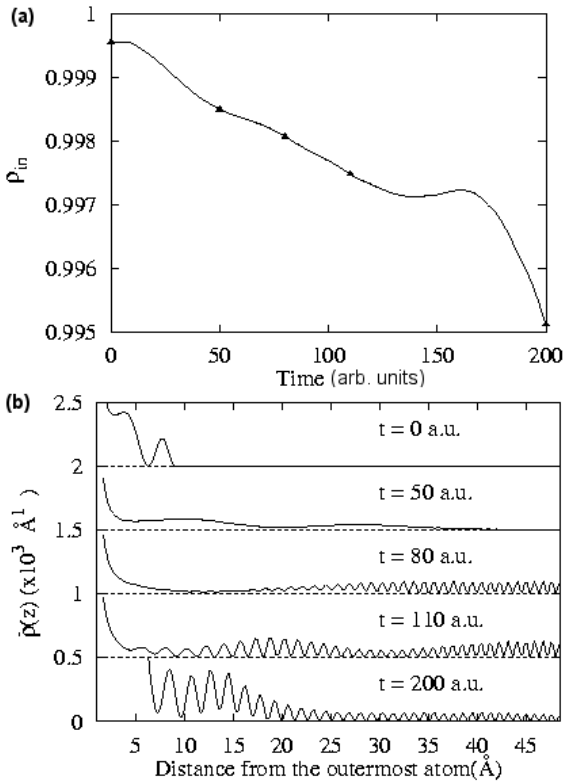


Fig. 1. Time-evolution of LUMO in the  $C_{12}H_2$  chain under the external field of  $1.0 \text{ V/\AA}$ . (a) The change of electron charge inside the tube ( $\rho_{in}$ ) as evaluated by integrating the density over  $z < z_0$ . (b) The snapshots of the  $xy$ -averaged densities at the points marked in (a).

adsorbates at the tip [12]. The contribution of the localized states increases for the nanostructures where the atomic size of the tip restricts the number of the conducting channels, but these localized states are not well described in the semi-classical approach.

In this article, we will first present the results of the first-principles calculation on the field emission of linear carbon chains, addressing the above-mentioned relevance of the realistic computation. We will then briefly report the calculation of the field emission from the curved or tilted carbon nanotubes in comparison with straight and vertical (upright) nanotubes. In our analysis of the field emission process, we do not make any simplifying assumptions on the geometry, potential distributions, or electronic states. We calculate the electronic structures of carbon chains and carbon nanotubes (under a given applied electric field) using the standard *ab initio* pseudopotential method [13] with the local density approximation. Troullier-Martins pseudopotentials [14] in the separable form are used with a cutoff energy 40 Ry to ensure the reliable computational results. When computing the potential driving the field emission, we have used pseudo-atomic-orbitals in the expansion of wave functions [15]. Suzuki-Trotter type split operator method [16] and the plane waves are used for tracing the electron

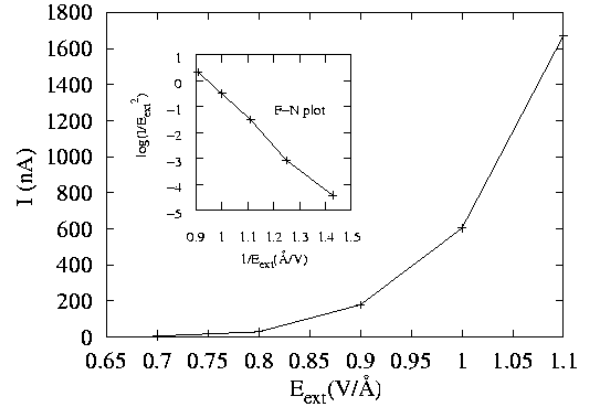


Fig. 2. Current-electric field characteristics of the carbon chain. The inset is the F-N plot.

motions. A saw-tooth type potential is applied for simulating the external electric field. Detailed procedures for the computations will be presented elsewhere [17].

In a unit supercell, we have 12 carbon atoms forming a linear chain with two hydrogen atoms attached at both ends. The H atoms saturate the dangling  $\sigma$ -bonds in the bare carbon chain, eliminating states near the Fermi level. Therefore, the current sources near the Fermi level are all extended  $\pi$ -states. The vacuum space is  $45 \text{ \AA}$  in length outside the carbon chain. The state right above (LUMO state) and below the Fermi level (HOMO state) are 3.9 and 5.8 eV below the vacuum level, respectively. Since the pseudo-atomic orbitals are slightly shrunk from the original atomic orbitals, the additional Coulomb energy may cause some error in the energy levels of each eigenstates.

At  $t = 0$ , the wave functions are confined within the emitter because the local the basis set is used. Upon changing basis to plane waves at  $t > 0$ , the electron starts to leak out of the carbon chain and the electron density in vacuum begins to increase. In order to evaluate the rate of electron leakage, we integrate the electron density inside the carbon chain ( $\rho_{in}$ ) over  $z_0 < z < z_1$ , with  $z_0$  and  $z_1$  effectively defining boundary planes that separate the carbon chain and the vacuum. In Fig. 1, the time-evolution of  $\rho_{in}$  is presented for the LUMO with the external field of  $1.0 \text{ V/\AA}$ . The time increment  $\Delta t$  in the time-displacement operator ( $e^{-iH\Delta t/\hbar}$ ) is set to 0.1 a.u. (1 a.u. = 0.0242 fs) and the operator is symmetrically decomposed up to the fourth order of  $\Delta t$  [18]. The integration boundaries  $z_0$  and  $z_1$  are fixed at  $3 \text{ \AA}$  outside the H atoms but the results are insensitive to the variations of  $z_0$  by an order of angstrom.

In order to investigate the detailed features of the evolution, we mark a filled triangle to the curve in Fig. 1(a) at the times when qualitative changes occur. The  $xy$ -averaged densities ( $\bar{\rho}(z)$ ) at these points are displayed in Fig. 1(b). Before  $t = 50$  a.u., the electron-leakage graph is quite linear, giving the transition rate in the emission process. Shortly after  $t = 50$  a.u., the tail of

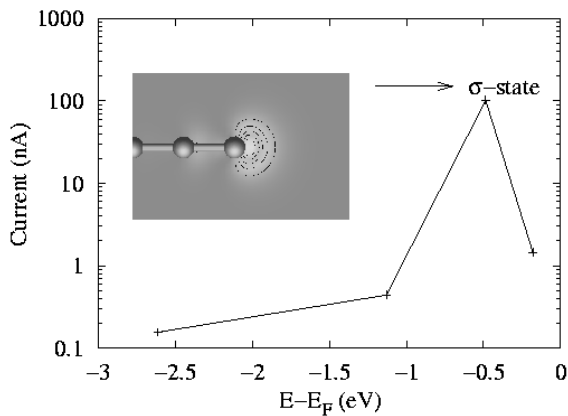


Fig. 3. Currents of the occupied states in a  $C_{12}$  chain under an external field of  $1.0 \text{ V/\AA}$ . The inset shows the dangling  $\sigma$ -bond that gives the largest current.

the wave function reaches the boundary of the supercell where a large barrier is present because of the saw-tooth type potential. The interference between the outgoing and reflected waves is shown as small wiggles at  $t = 80$  a.u. The reflected wave begins to flow backward into the carbon chain around  $t = 110$  a.u. Finally, the resonance occurs near the end of our simulation (Rabi oscillation) and large changes in  $\rho_{in}$  are observed. To avoid such a computational artifact, we take the slope around the  $t = 50$  a.u. as the transition rate of the state. It is found that the initial time region showing the linear behavior can be extended by adopting a longer supercell, consistent with the above analysis.

The current for each state is evaluated by multiplying the electron charge, the transition rate, and the occupation number. Each level is doubly degenerate due to the rotational symmetry of the carbon chain. The magnitude of the current contributed by each state is exponentially dependent on the energy level. Due to the exponential decay of the current to the low energy side, it is sufficient to consider only the states within  $\sim 2$  eV below the Fermi level. Figure 2 shows the calculated  $I$ - $E$  curves for the carbon chain. The exponential growth of the current can be seen and the F-N plot presented in the inset is linear as predicted by the classical formula. This indicates that the F-N formula would provide a useful functional form for the data fitting, although F-N theory may not be valid at the atomic scale. In the usual situation, the field emission occurs when the local electric field is  $\sim 1 \text{ V/\AA}$ . Under such electric fields, Fig. 2 indicates that the emission current of hundreds of nanoamperes is extracted from the carbon chains, in good agreements with the amount of the current observed in the experiment of Rinzler *et al.* [6]. If the chain is extended to include more carbon atoms, the density of the state will increase. However, the transition rates are reduced because of the smaller amplitude near the vacuum and the total amount of current will remain the same provided that the local electric field is identical.

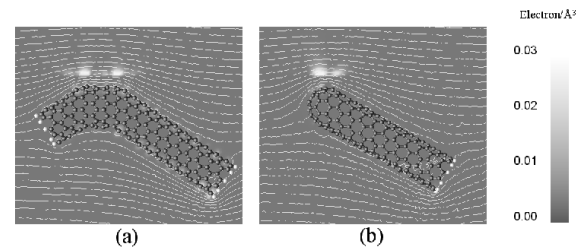


Fig. 4. Self-consistent potential around the nanotube and the charge distribution of the emitted electron. The applied electric field is  $0.7 \text{ V/\AA}$  and the charge distribution is a snapshot taken at  $10^{-15}$  s after the initiation of the tunneling. The spacing between the equipotential lines is 1 volt. (a) and (b) are for curved  $(5,5)/(9,0)/(5,5)$  and  $60^\circ$  tilted  $(5,5)$  nanotubes, respectively. For visual purposes, the electron density on the vacuum side is magnified by  $10^4$ .

As another model, we detach the passivating H atoms, exposing the dangling  $\sigma$ -bond at the end of the chain. The currents for individual states are shown in Fig. 3. A notable feature is that the dangling-bond state at the front of the emitter [inset of Fig. 3] generates a pronounced current even though it is not the closest state to the Fermi level. According to the Fermi golden rule, the transition rate of a state depends on the transfer integral between the initial and the final states. The vacuum states coupled to the  $\pi$ -states should have the same angular momentum in  $xy$  plane as that of the  $\pi$ -states. The phase variation acts as an additional barriers along the  $z$ -direction and the overlap integral between the  $\pi$ -states and the vacuum state is reduced. On the other hand, the dangling bond with a  $\sigma$  character has no node in the plane perpendicular to the emission direction and the coupling to the vacuum state is enhanced, resulting in a large current. In addition, this state protrudes to the vacuum region and experiences the smallest barrier thickness among all states. This demonstrates that the spatial distribution as well as the energy level is a critical factor for the transition rate. The current of the  $\pi$ -states is suppressed because of the increase in the work function ( $\pi$ -states in this geometry lie at lower energy than in other cases) and the total current of the  $C_{12}$  chain is about a quarter of the value of the  $C_{12}H_2$  chain.

We have also studied the field emission from the curved or tilted carbon nanotubes. Figure 4(a) and 4(b) show the potential profile and the charge distribution around the curved and tilted (by  $60^\circ$ )  $(5,5)$  nanotubes. The charge is summed over the states contributing to the current. The emission area more or less spreads over the body (side wall) of the nanotube. Emission currents of curved and tilted tubes turn out to be a few percent of the straight and vertical nanotube of the same size. Effective local fields experienced by the electrons are reduced because of the smaller aspect ratio and oblique geometries. The turn-on voltage for emission is inversely proportional to the field enhancement factor, and our

calculation indicates that the emission from the favorable geometry (straight and vertical) occurs at  $\sim 60\%$  of the bias voltage necessary to turn on the unfavorable tubes shown in Fig. 4(a) and 4(b). In other words, at the bias voltage necessary for the practical current density, only a small number of nanotubes of favorable geometry emit electrons. This is actually what was observed in the experiment where the density of the bright points on the screen was not more than  $10^4/\text{cm}^2$  [19], corresponding to roughly one active tube out of 10000. On the other hand, if we are able to increase the uniformity of the tubes significantly and make 1% of the total number of tubes emit, not only would the uniformity of the screen brightness improve greatly, but the threshold voltage could further drop by  $\sim 30\%$  according to our simulation.

Another issue we have not dealt with is the effect of the bundle of nanotubes. The bundle may develop a pseudogap in the electronic structure of an originally metallic nanotube [20], which will increase the resistance of the nanotube emitter. Also, the field enhancement factor will be significantly reduced. Both effects would be harmful to the performance of the field emission.

In conclusion, we have performed first-principles calculations on the field emission of linear carbon chains and the curved or tilted carbon nanotubes. The magnitude of the computed current accounts well for the experimental observations. Because of the exponential dependence of the current on the energy level, only a small portion of the states near the Fermi level contributes to the current. It is demonstrated that three-dimensional shapes of the sources and the existence of localized states are important factors determining the emission current from nanostructures.

#### ACKNOWLEDGMENTS

This work was supported by the BK21 project of the KRF, the Ministry of Information and Communication of Korea, and Samsung Electronics. The computation were carried out on the CrayT3E of the KISTI Supercomputing Center.

#### REFERENCES

- [1] S. Iijima, *Nature* **354**, 56 (1991).
- [2] W. B. Choi, D. S. Chung, J. H. Kang, H. Y. Kim, Y. W. Jin, I. T. Han, Y. H. Lee, J. E. Jung, N. S. Lee, G. S. Park and J. M. Kim, *Appl. Phys. Lett.* **75**, 3129 (1999).
- [3] H. Schmid and H. W. Fink, *Appl. Phys. Lett.* **70**, 2679 (1997).
- [4] J.-M. Bonard, J.-P. Salvetat, T. Stockli and W. A. de Heer, *Appl. Phys. Lett.* **73**, 918 (1998).
- [5] P. G. Collins and A. Zettl, *Phys. Rev. B* **55**, 9391 (1997).
- [6] A. G. Rinzler, J. H. Hafner, P. Nikolaev, L. Lou, S. G. Kim, D. Tomanek, P. Nordlander, D. T. Colbert and R. E. Smalley, *Science* **269**, 1550 (1995)
- [7] L. Lou and P. Nordlander, *Phys. Rev. B* **54**, 16659 (1996).
- [8] A. Lorenzoni, H. E. Roman, F. Alasia and R. A. Broglia, *Chem. Phys. Lett.* **276**, 237 (1997).
- [9] Y. Saito, K. Hamaguchi, K. Hata, K. Uchida, Y. Tasaka, F. Ikazaki, M. Yumura, A. Kasuya and Y. Nishina, *Nature* **389**, 554 (1997).
- [10] J. He, P. H. Cutler and N. M. Miskovsky, *Appl. Phys. Lett.* **59**, 1644 (1991).
- [11] M. S. Chung, I. W. Kim, J. M. Park and P. H. Cutler, *J. Korean Phys. Soc.* **30**, S198 (1997).
- [12] J. W. Gadzuk and E. W. Plummer, *Rev. Mod. Phys.* **45**, 487 (1973).
- [13] J. Ihm, A. Zunger and M. L. Cohen, *J. Phys. C: Solid State Phys.* **12**, 4409 (1979).
- [14] N. Troullier and J. L. Martins, *Phys. Rev. B* **43**, 1993 (1991).
- [15] O. F. Sankey and D. J. Niklewski, *Phys. Rev. B* **40**, 3979 (1989); D. A. Drabold, R. Wang, S. Klemm, O. F. Sankey and J. D. Dow, *Phys. Rev. B* **43**, 5132 (1991).
- [16] M. Suzuki, *J. Phys. Soc. Jpn.* **61**, L3015 (1992); M. Suzuki and T. Yamauchi, *J. Math. Phys.* **34**, 4892 (1993).
- [17] S. Han and J. Ihm, to be published in *Phys. Rev. B*.
- [18] O. Sugino and Y. Miyamoto, *Phys. Rev. B* **59**, 2579 (1999).
- [19] W. Zhu, C. Bower, O. Zhou, G. Kochanski and S. Jin, *Appl. Phys. Lett.* **75**, 873 (1999)
- [20] P. Delaney, H. J. Choi, J. Ihm, S. G. Louie and M. L. Cohen, *Nature* **391**, 466 (1998).